

Neutralization Effect on Energetic Proton Confinement in LHD

SASAO Mamiko[†], KRASILNIKOV Anatolii V.¹, ISOBE Mitsutaka, SEKI Tetsuo, SAITO Kenji,
SAIDA Tomoya, MURAKAMI Sadayoshi and the LHD-Experimental Group
National Institute for Fusion Science, Toki 509-5292, Japan

¹ Troitsk Institute for Innovating and Fusion Research (TRINITI), Troitsk, Russia

(Received: 14 December 2001 / Accepted: 24 June 2002)

Abstract

The neutralization effect for energetic protons in Large Helical Device (LHD) was estimated from the high energy neutral flux measured by Natural Diamond Detectors (NDD). The neutral- and partially-ionized-particle-distributions are calculated with a code for the incoming H^0 , He^0 transport (Analytical Calculation of Helium Neutral, ACHEN-Code). The electron density dependence of the effective He^+ density at the ICRF resonance region derived from measured neutral flux of high energy particles is well reproduced by the neutral-transport calculation with the incoming neutral temperature of about 10 eV and the neutral density at the Last Closed Flux Surface (LCFS) of $10^{-3} \times n_e$. The estimated loss rates are consistent in factors with the saturation level of decaying time of tail temperature after the termination of the ICRF heating.

Keywords:

Neutralization, High-energy particle, High energy tail, Large Helical Device, Diamond Detector, ICRF-heating, Neutral particle

1. Introduction

In Large Helical Device (LHD), high-energy neutral flux and spectra are measured by Natural Diamond Detectors (NDD) [1], Si-diodes [2], and conventional Neutral Particle Analyzers (NPA) [3], during NBI sustained, ICRF sustained, or ICRF assisted NBI discharges. With a help of a code to calculate H^0 , He^0 , He^+ distribution (ACHEN-Code) [4], the effective temperature, T_{eff} , of an energetic tail formed by ICRF-waves is obtained for most of ICRF discharges since the 3rd Champaign [5-7]. Comparison of measured effective perpendicular temperature of ICRF driven H^+ minority ions with the classical Stix model indicates that

perpendicular ions are well confined in the center region of the LHD. However, deviation from the classical prediction was observed in the outer region of the plasma, indicating ripple-induced transport and charge-exchange-losses [7]. In separate experiments, the relaxation time (t_{decay}) of T_{eff} in decaying phase after ICRF termination is studied. It is consistent with the classical prediction when $t_{\text{decay}} < 0.1\text{sec}$, but it saturates at around 0.15–0.2 sec, indicating existence of loss which has a time constant of this range [6].

Among various loss mechanisms of high-energy ions in magnetically-confined fusion plasma, neutralization loss is one of the key processes. This is

Corresponding author's e-mail: sasao@nifs.ac.jp

[†] Present address: Department of Quantum Science & Energy Engineering,

Graduate School of Engineering, Tohoku University, Sendai 980-8579, Japan.

sasao@qse.tohoku.ac.jp

©2002 by The Japan Society of Plasma Science and Nuclear Fusion Research

loss of energetic particles that are neutralized through charge exchange processes with residual neutrals or partially ionized ions in a plasma. The magnitude of this contribution is strongly related to their orbits, because excursion from the magnetic flux surface to outer region where the neutral density is higher, enhances the neutralization probability.

In the present work, the neutralization effect has been studied by analyzing the high energy neutral flux of a vertical viewing chord measured by NDD during ICRF-heating experiments. Here the discharge gas is helium with small amount of H-minority. The measured neutral flux is compared with that estimated from the density of protons which are coupled with ICRF, and neutral and partially-ionized particle density in a core plasma. The latter is calculated using a code to calculate H^0 , He^0 , He^+ distribution (ACHEN-Code). Once the calculated H^0 , He^0 , He^+ density distributions and source neutral temperature are verified, it is possible to evaluate the total neutralization loss.

2. Experimental Setup and Data Analysis

Two sets of NDD of vertical line of sight are used in the present work [4]. Each detector assemble has a double slit system, but the geometrical efficiency, η_g and the viewing area, s are determined by the detector size (2 mm) and the changeable aperture of 525 mm apart. The aperture of the center chord, which provides most of measurement of present study was fixed at 2mm ($\eta_g = 1.53 \times 10^{-7}$, $s = 2 \times 10^{-4} \text{ m}^2$). The details of the measurement setup are discussed in ref. 1.

A simplified relation [6] of measured neutral flux,

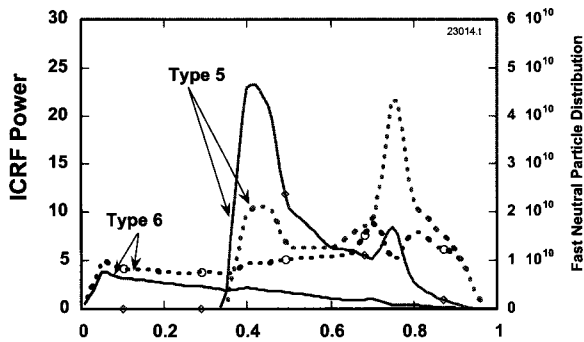


Fig. 1 ICRF power deposition profiles of 38.47 MHz (type-5) and of 40.47 MHz (type-6) at $B_t = 2.75 \text{ T}$, $R_x = 3.6 \text{ m}$ are shown by solid lines. Dotted lines indicate those multiplied by the $n_{He^+}(z)$ profile calculated with $T^0 = 10 \text{ eV}$, and $n^0 = 10^{-3} \times n_e$, where $n_e = 1 \times 10^{13}/\text{cm}^3$.

$\Gamma_{\text{meas}}(E)$ to the proton energy distribution function $f_p(E)$ that separates the z -dependent and E -dependent factors,

$$\Gamma_{\text{meas}}(E) \approx \eta_g s g(E) f_p(E) \int n_p(z) n_{He^+}(z) dz. \quad (1)$$

has been used for the analysis. Here z is a vertical coordinate along the viewing line. In the present study, we consider H^0 , He^0 , and He^+ , as particles responsible for the neutralization, but the contribution of the He^+ is most important, so we use the profile of He^+ but the energy dependence of the sum of all contributors. We first calculate the z -dependent factor, $n_p(z) n_{He^+}(z)$, and integrate along the line of sight, by using the calculated He^+ profile ($n_{He^+}(z)$) and the ICRF power deposition profile normalized in to 14 % proton density ($n_p(z)$), because the comparison of measured effective perpendicular temperature with the classical Stix model indicates that 14 % of total protons resonate to the ICRF waves [8]. The $n_{He^+}(z)$ profile depends on the neutral temperature T^0 , across LCFS and its density n^0 . These parameters are discussed in the next section. Examples of z -dependence are shown in Fig. 1. The velocity (energy) dependent factor $g(E)$ is neutralization efficiency and is summation of contributions from all possible atoms/ions (denoted as i), that can transfer one electron to a proton.

$$g(E) = \sum_i \langle \sigma^i v \rangle_E n_i(z_R) / n_{He^+}(z_R). \quad (2)$$

We consider only H^0 , He^0 , and He^+ , because the impurity concentration is low in LHD. Here z_R is a representative point through the viewing line, such as the resonance point of the ICRF wave. Finally the derived proton spectrum, $f_p(E)$ is fit into an exponential line,

$$f_p(E) dE \approx v_{\perp} dv_{\perp} [(m/2)^{1/2} (T_{\perp})^{-1/2} \exp\{-(mv_{\perp}^2/2)/T_{\perp}\}], \quad (3)$$

assuming that the parallel velocity distribution is that of thermal ions.

3. The Incoming Neutral Temperature and the Neutral Density

In the procedure to derive the effective perpendicular temperature T_{\perp} , the calculated He^+ profile ($n_{He^+}(z)$) is assumed. However this calculation contains two free parameters, the neutral temperature T^0 , incoming across LCFS and its density n^0 . The electron density dependence of n_{He^+} at certain radius inside the plasma core is determined by T^0 , while the overall absolute value is affected by n^0 . Some examples of time traces of ICRF sustained discharges of LHD at $B_t = 2.64 \text{ T}$, $R_x = 3.75 \text{ m}$, are shown in Fig. 2, together with those

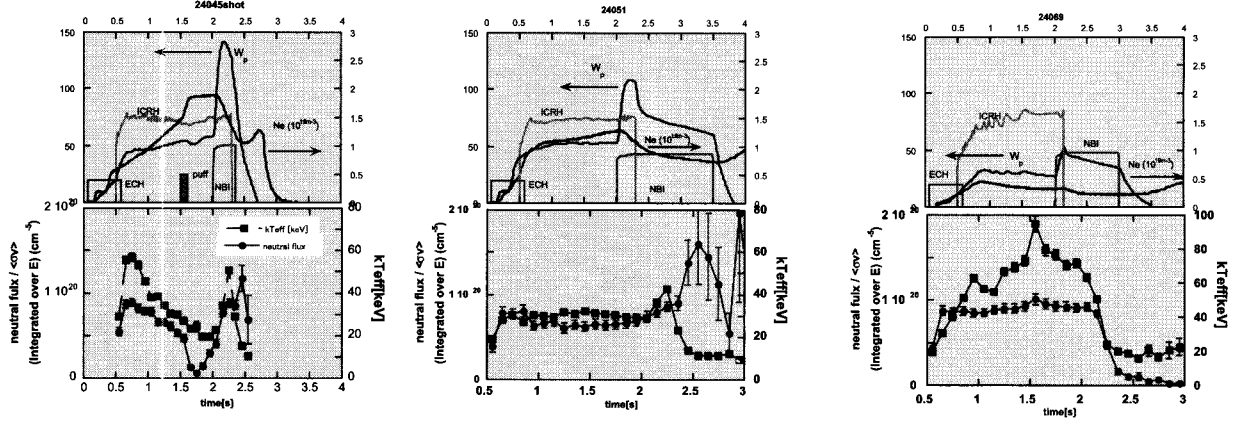


Fig. 2 Time traces of ICRF sustained discharges (#24045, 24051, 24069) of LHD at $B_t = 2.64$ T, $R_x = 3.75$ m, together with those of T_{\perp} and measured neutral flux Φ . The minority concentration is kept nearly constant (7%) while the electron density varies from $0.3 \times 10^{13}/\text{cm}^3$ (#24069), $1 \times 10^{13}/\text{cm}^3$ (#24051) to $2 \times 10^{13}/\text{cm}^3$ (#24045), and T_{\perp} are changing accordingly. Note that the neutral beams are injected after $t=2$ sec, and short but strong gas puffing at 1.5 sec on #24045.

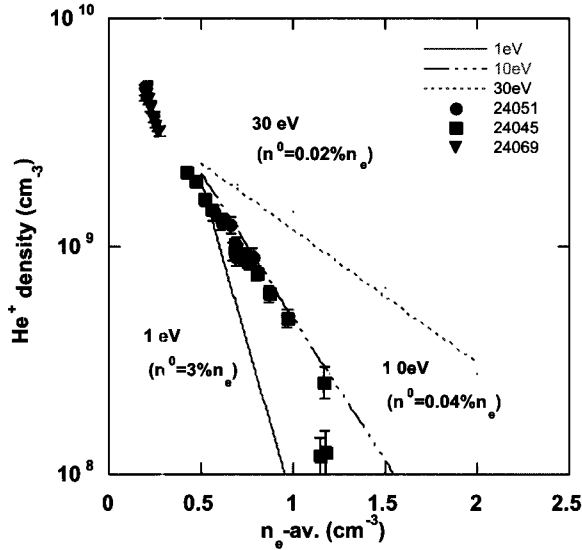


Fig. 3 The electron density dependence of $n_{\text{He}^+}(z)$ estimated from Φ upon n_e (symbols). The lines are those calculated at $\rho = 0.5$, where the ICRF resonance surface exists. Good agreement is obtained by the neutral-transport calculation with $T^0 = 10$ eV and $n(\text{neutral})/n_e = 4 \times 10^{-4}$.

of T_{\perp} , and measured neutral flux Φ , which is the measured proton spectra integrated over E, defined by

$$\Phi = \int \Gamma_{\text{meas}}(E)/g(E) dE \quad (4a)$$

$$\approx \eta_g s \int n_p(z) n_{\text{He}^+}(z) dz. \quad (4b)$$

As the electron density varies from $2 \times 10^{13}/\text{cm}^3$ (#24045), $1 \times 10^{13}/\text{cm}^3$ (#24051) to $0.3 \times 10^{13}/\text{cm}^3$

(#24069), both T_{\perp} and Φ are increasing. The dependence of He^+ density estimated from Φ upon n_e (Fig. 3) is compared with the calculated $n_{\text{He}^+}(z)$ at $\rho = 0.5$, where the ICRF resonance surface exists, for three cases of T^0 , (30 eV, 10 eV, 1 eV). As the T^0 is diminished, the attenuation of neutrals become severe, and the He^+ density decreases. Good agreement is obtained for $T^0 = 10$ eV. The absolute value of $n_{\text{He}^+}(z)$ and hence n^0 can be obtained from Φ by normalizing it with $\eta_g s \int n_p(z) n_{\text{He}^+}(z) dz$ calculated for each T^0 , thus obtained. In the present case, the n^0 of $0.4 \times 10^{-3} n_e$, obtained with $T^0 = 10$ eV is consistent with the measured density dependence.

4. Neutralization Loss and Conclusion

High-energy neutral particles detected are actually particles lost from the plasma, and directly related to the neutralization loss. The local information on the neutralization loss and its energy dependence can be estimated by using the T^0 and n^0 derived from the comparison of the density dependence and absolute neutral flux with the calculation. Using these parameters obtained in the analysis described in the previous section (with $T^0 = 10$ eV, $n^0 = 0.4 \times 10^{-3} n_e$), and the neutralization loss profiles are estimated as in Fig. 4. Here, we used the effective neutralization probability of $g(E)$ as defined in eq. (2), including three charge exchange rates. A short neutralization time causes large neutralization loss. Figure 4 indicates that the neutralization loss is not negligible when the density is less than $10^{13}/\text{cm}^3$ in the peripheral region ($\rho > 0.7$), especially

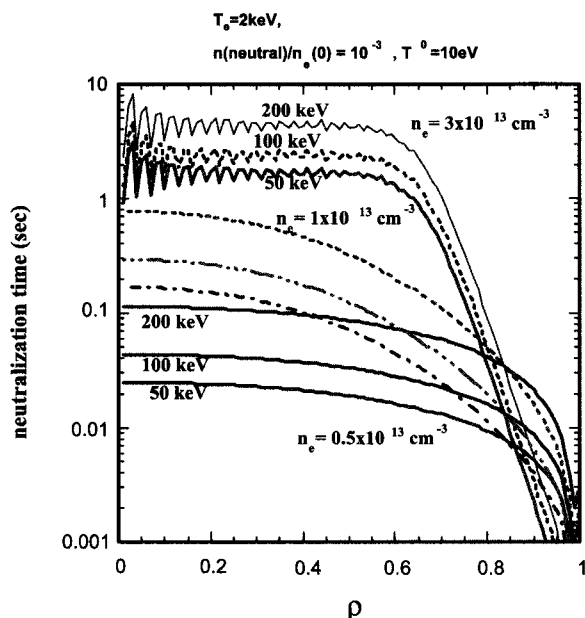


Fig. 4 The neutralization loss time estimated at the electron density of $0.5 \times 10^{13}/\text{cm}^3$, $1 \times 10^{13}/\text{cm}^3$ and $3 \times 10^{13}/\text{cm}^3$ of helium plasma for energetic protons of 50 keV, 100 keV, and 200 keV, when $n(\text{neutral})/n_e = 4 \times 10^{-4}$, and $T^0 = 10 \text{ eV}$.

for ions in the energy about 50 keV. When the electron density is $1 \times 10^{13}/\text{cm}^3$, the characteristic neutralization time at the ICRF resonance region ($0.4 < \rho < 0.7$) is 40 – 200 ms, which is consistent with the saturation level of decaying time (150 – 200 ms) of tail temperature after the ICRF termination [6], indicating that the neutralization is one of the dominant loss

processes. However, the present calculation shows that particles of energy higher than 100 keV have longer confinement time, while the saturation in the Stix diagram shows the faster loss for higher-energy particles.

In this study, the orbit effect that the excursion of high-energy particle orbit from the magnetic flux surface is not considered. Actually this effect is strongly coupled to the neutralization loss, and affects more for higher energy particles. The study on the combined effect of orbit excursion and neutralization is now in progress.

References

- [1] Isobe M., Sasao M., Iiduka S., Krasilnikov A.V. *et al.*, *Rev. Sci. Instrum.* **72**, 611 (2001).
- [2] Osakabe M. *et al.*, *Rev. Sci. Instrum.*, **72**, 788 (2001).
- [3] Ozaki T. *et al.*, *Rev. Sci. Instrum.* **71**, 2698 (2000).
- [4] M. Sasao *et al.*, Proc. "Advanced Diagnostics for Magnetic and Inertial Fusion", (Varenna, 2001), edited by P.E. Stott *et al.* (Plenum Press, New York), p129 (2002).
- [5] Mutoh, T. *et al.*, *Phys. Rev. Lett.* **85**, 4530 (2000).
- [6] Sasao M. *et al.*, in Fusion Energy 2000 (Proc. 18th Int. Conf., Sorrento, 2000), IAEA, Vienna (2001) CD-ROM file EX9/1 .
- [7] Krasilnikov A.V. *et al.*, *Nucl. Fusion* **42**, 759 (2002).
- [8] Saito, K. *et al.*, *Nucl. Fusion*, **41**, 1021 (2001).